



Climatology, Variability, and Trend of the Winter Precipitation over Nepal

Binod Dawadi^{1,2,3} · Shankar Sharma¹ · Emmanuel Reynard^{3,4} · Kabindra Shahi⁵

Received: 2 June 2022 / Revised: 22 December 2022 / Accepted: 4 January 2023 / Published online: 24 January 2023
© King Abdulaziz University and Springer Nature Switzerland AG 2023

Abstract

Winter precipitation accounts for ~5% of interannual spatial variability during the last five decades (1960–2015), with the largest variability in the western and central regions of Nepal. The temporal variability shows a relatively higher degree of variability after the 1990s. In this study, the dominant modes of winter precipitation pattern, trend and their association with oceanic and atmospheric patterns were investigated over the southern slope of the central Himalaya, Nepal. The increasing trend (< 1 mm/year) of winter precipitation is found only over the highlands of the western and central regions, whereas decreasing trend or no trend in most of the areas over the country. Further, two dominant modes of winter precipitation were observed through Empirical Orthogonal Function (EOF) analysis. The first leading mode (EOF1) shows a monopole pattern with 42.9% variability with strong loading over the western and central regions, whereas the second mode (EOF2) shows a heterogeneous pattern, accounting for 18.9% of the total variance. Further, the EOF1 pattern is remotely influenced by El Niño-Southern Oscillation (ENSO) and locally through Indian Ocean Basin Mode (IOBM) patterns. It is also observed that the EOF2 mode has a close relationship with the North Atlantic Oscillation (NAO), modulating the wave train and propagating eastward to the western Himalayas.

Keywords Winter precipitation · EOF · Oceanic pattern · Nepal

1 Introduction

Nepal is located on the southern slope of the Central Himalayas (Fig. 1) and receives its winter (December–January) precipitation due to the influence of western disturbances (Wang et al. 2013). These Himalayas acts as a wind barrier, moisture from the westerly jet stream directs the passage of extratropical storms (western disturbances, WD) through

northwestern India and Nepal (Hasson et al. 2014; Hunt and Zaz 2022; Mehmood et al. 2022). The moisture from the Arabian Sea, western Indian Ocean (IO), Atlantic Ocean and other terrestrial, and oceanic sources (Dimri 2013a, 2013b; Kamil et al. 2019; Syed et al. 2010) enters Nepal from the western region with a high amount of precipitation in western hills and decreases toward central and eastern regions (Hamal et al. 2020a). Although winter precipitation accounts for only ~3% of the annual precipitation (Sharma et al. 2021); however, the interannual variability of the winter precipitation often initiates extreme events (i.e., drought, flash flood) (Kar and Rana 2014), affecting agriculture, and overall socio-economic condition of the country. For example, during the drought in 2008/2009, the deficient precipitation in western Nepal impacted the groundwater resources and the winter crop yield (Dimri 2013a; Hamal et al. 2020b; Wang et al. 2013), leading to huge economic loss and food insecurity. Similarly, Barlow et al. (2002) found that warm ocean waters in the western Pacific appear to be a major reason for severe drought during 1998–2001, which has led to widespread starvation affecting over 60 million people in central and southwest Asia. On the other hand, winter

✉ Binod Dawadi
dawadib@cdhmtu.edu.np

¹ Central Department of Hydrology and Meteorology, Tribhuvan University, Kirtipur, Kathmandu 44613, Nepal
² Kathmandu Center for Research and Education, Chinese Academy of Sciences-Tribhuvan University, Kirtipur, Kathmandu 44613, Nepal
³ Interdisciplinary Center for Mountain Research, University of Lausanne Switzerland, Lausanne, Switzerland
⁴ Institute of Geography and Sustainability, University of Lausanne, Lausanne, Switzerland
⁵ Sri Dev Suman Uttarakhand University Badshahthaul Tehri Garhwal (SDSU), Chamba, Uttarakhand, India

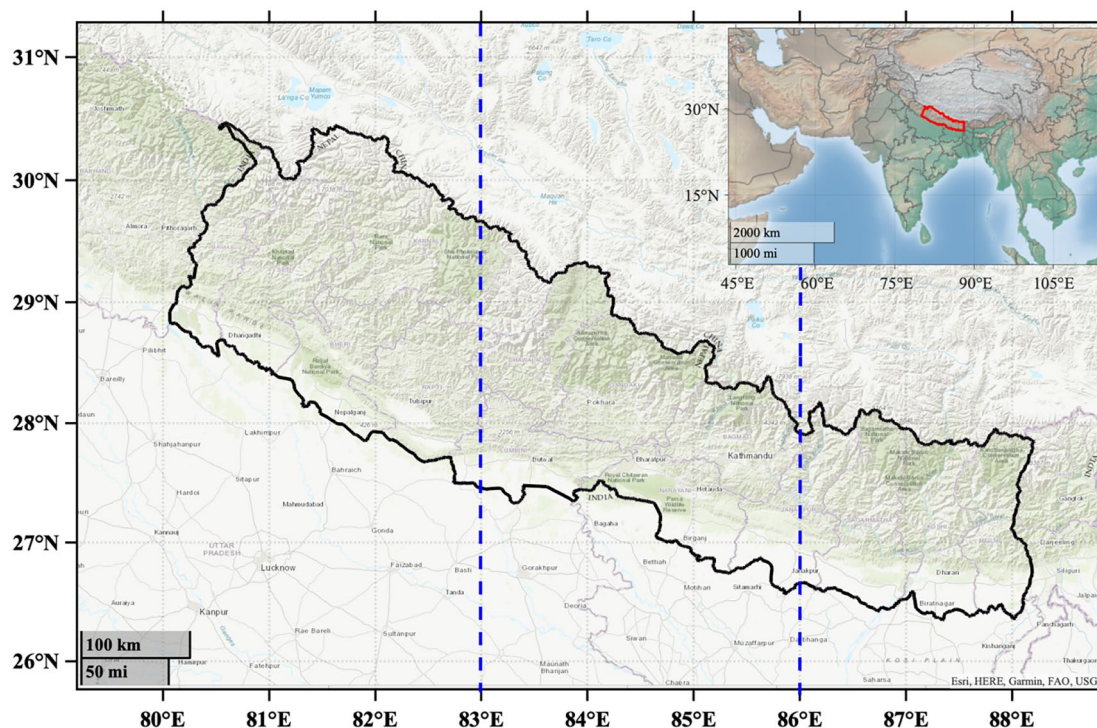


Fig. 1 Study area Nepal. Blue dot lines separate the Western (western boundary to 83°E), Central (from 83° to 86°E), and Eastern region (from 86°E to eastern boundary)

precipitation also plays a major role in glacier mass balance, whereas Liu and Chen (2000) found the greatest warming trend during winter season over the northern slope of Central Himalayas. Further, the ongoing climate change can worsen these warming and extremes (Huber and Gullede 2011). Therefore, in this paper, we aim to explore the long-term (last five decades; 1960–2015) variability of winter precipitation over Nepal.

The oceanic pattern and atmospheric circulation play an essential role in climate variability (Liu et al. 2020; Mishra et al. 2012; Niranjana Kumar et al. 2013; Sharma et al. 2020a; Wang et al. 2013). For example, Mehmood et al. (2022) found that mid-latitude regions, including the Mediterranean/Caspian Seas and Mediterranean land, contribute significant moisture to the cold season precipitation over the high mountains of Asia and surrounding areas. The authors also mentioned the fluctuating influence on precipitation distribution due to the tropical and extratropical forcings. Previous studies have also shown the significant influence of below-normal and above-normal equatorial IO Sea Surface Temperature (SST) on the climate of Nepal (Hamal et al. 2020a; Pokharel et al. 2019; Sharma et al. 2020a). The natural phenomena that have robust control over the winter precipitation at interannual timescale are the El Niño/Southern Oscillation (ENSO), the North Atlantic Oscillation (NAO), and Indian Ocean

Basin Mode (IOBM) (Dimri 2013b; Kar and Rana 2014; Liu et al. 2020; Zhang et al. 2015). Further, several studies have found a strong relationship between the ENSO and winter precipitation over the Himalayan region (Hamal et al. 2020a). During the warm phase of ENSO, the cyclonic circulation observed at the upper level over Northern India intensifies the western disturbances passing through it (Dimri 2013b; Yadav et al. 2013). However, the shift in the influence of ENSO on winter precipitation has been observed before and after 1979, resulting in significant variation of winter precipitation over the northwestern part of India (Yadav et al. 2010). As NAO significantly influences the WD, its effect on winter precipitation is also strong, especially during the positive phase (Hunt and Zaz 2022), which further intensifies the western disturbances (Syed et al. 2006); however, the diminishing role of the NAO on the winter precipitation in the Himalayan region has also been observed (Yadav et al. 2009). Moreover, the basin-wide warming/cooling of the IO affects the winter precipitation, which often accompanies the ENSO (Liu et al. 2020), through the atmospheric circulation (Hamal et al. 2020a). Further, The Tropical Western-Eastern Indian Ocean dipole can propagate the ENSO influence over the Central South Asian regions by inducing changes in the atmospheric circulations through atmospheric diabatic heating anomalies (Abid et al. 2020). Therefore, this

study aims to understand the ENSO, IOBM, and NAO influence on the dominant pattern of winter precipitation variability over Nepal.

2 Data and Methodology

We have used a newer version of $0.25^\circ \times 0.25^\circ$ gridded APHRODITE (Asian Precipitation Highly Resolved Observational Data Integration toward Evaluation of the Water Resources) data over monsoon Asia (APHRODITE-1 and APHRODITE-2) from 1960 to 2015. The APHRODITE is a gage-based gridded dataset developed from a dense network of rain gage stations (stations from the monsoon Asia region) in conjunction with other pre-compiled datasets (Yatagai et al. 2009, 2012). While generating this dataset, it uses the maximum possible gages available over Nepal (Yatagai et al. 2009). Further, Sharma et al. (2020a) validated the APHRODITE precipitation dataset with the observed data from 220 meteorological stations (1987–2015) across Nepal, showing a strong correlation of 0.93, and suggested APHRODITE as the best alternative to gage observation for Nepal. Following previous studies (Chen 2021; Sharma et al. 2020a, 2020b), the study area Nepal is divided into three regions, i.e., Western (western boundary to 83°E), Central (from 83° to 85°E), and Eastern region (from 85°E to eastern boundary) based on three major river basins and monsoonal climatology (Fig. 1). In addition to APHRODITE, ERA5 reanalysis datasets have also been used to analyze the spatial trend of the winter precipitation between 1960 and 2015 over Nepal. ERA5 is fifth generation of the European Reanalysis (C3S 2017), which provides precipitation at a $0.25^\circ \times 0.25^\circ$ horizontal grid spacing and at an hourly timescale, which are temporally averaged to generate monthly means.

The teleconnection between winter precipitation and the oceanic pattern was assessed using the long-term monthly SST. The SST data were obtained from the National Oceanic and Atmospheric Administration (NOAA). Similarly, the zonal and meridional winds at 500 hPa were taken from the National Centers for Environmental Prediction/National Center for Atmospheric Research (NCEP/NCAR) reanalysis to resolve the atmospheric circulation. Moreover, the monthly oceanic climatic indices NINO3.4 and North Atlantic Oscillation (NAO) were downloaded from <https://www.psl.noaa.gov/data/climateindices/list/>. The Indian Ocean Basin Mode (IOBM) is then calculated from SST within 40°E – 120°E and 20°S – 20°N (Lu et al. 2019).

The different spatial patterns of the winter precipitation over Nepal with their time series and percentage of variance were calculated using an empirical orthogonal function (EOF) (Sein et al. 2015; Wang et al. 2015a). EOF analysis is a computation of the different Eigenmodes for a covariance matrix based on precipitation providing spatio-temporal

pattern as well as the percentage of variance. In this study, two dominant modes (EOF1 and EOF2; as the first two modes represent more than 60% of the variance) and their associated Principal Components (PC1 and PC2) were selected to determine the dominant mode of winter rainfall over the study area. The eigenvalues express the importance of the EOFs/Principal Components (PCs), whereas the first EOF (EOF1) is crucial, followed by the second EOF (EOF2), and so on (Wang et al. 2015b). More theories and algorithms details about EOF and PCs can be accessed from Lorenz (1956) and Zhang and Moore (2015). The Standard Deviation (SD) is calculated to show the spatial variation of winter precipitation over the study region. The higher (lower) value of the SD indicates the larger (smaller) spatial variability. Further, we introduce a stream function to consider the wind field divided into rotational and divergent components. The rotational component of geostrophic winds flows parallel to the contours of stream function, i.e., high (low) stream function corresponds to high (low) geopotential height in the Northern Hemisphere and to low (high) geopotential height in the Southern Hemisphere (Dey and Döös 2019). Additionally, the correlation analysis was carried out to understand the physical mechanism responsible for Oceanic, atmospheric, and precipitation change at a 90 and 95% confidence interval.

3 Results and Discussion

3.1 Climatology, Spatial and Interannual Variability

The long-term mean monthly cycle and climatology of winter precipitation from 1960 to 2015 are presented in Fig. 2. Monthly cycle of precipitation during the study period shows that winter precipitation accounts for only $\sim 5\%$ (46 mm) of the annual precipitation, whereas, post-monsoon, pre-monsoon, and monsoon seasons account for about 8%, 15%, and 72%, respectively (Fig. 2a). As the moisture from polar westerlies gets intensified when it reaches northern India, bringing the subtropical westerly jet streams ever closer to Nepal (Nayava 1980) and these westerly weather systems brings winter precipitation to the northwest mountains of the country. Further, the spatial distribution of winter precipitation in Fig. 2a shows that the highest (lowest) winter precipitation about 165 (30) mm over the mid-hills of the western (eastern) region of the country. The study region features unique topography (flatlands, Himalaya, and high-Himalaya within the 200 km range), which act as wind barriers that obstruct the movement of moist air eastward (Kansakar et al. 2004); thus, more precipitation falls in the northern part of western Nepal than in the south and much of falls as snow. There is also a decrease from west to east (highest in western region and lowest in eastern region). The

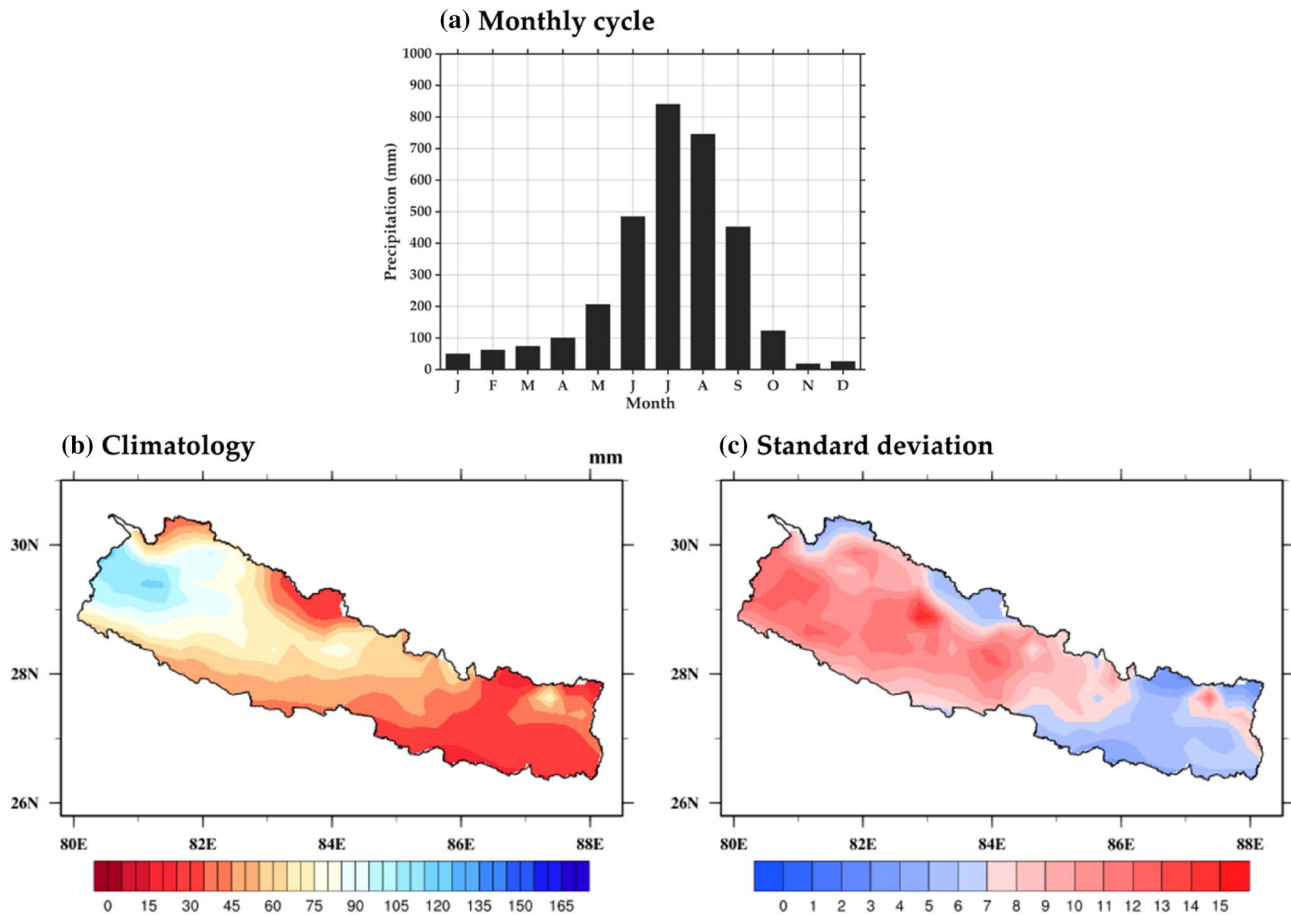


Fig. 2 a Mean monthly cycle, b climatology (unit: mm) and c the standard deviation of winter precipitation over Nepal for the period 1960–2015

mean winter precipitation in the western, central, and eastern regions are 80 mm, 55 mm, and 35 mm, respectively, during 1960–2015. It is worth noting that the mean precipitation in the low and mid-elevation of the eastern region and the Manang and Mustang district (rain shadow areas) of the central region have less than 30 mm. Previously, Hamal et al. (2020a) have also shown similar characteristics of the winter precipitation over Nepal.

Further, we examined the standard deviation of the winter precipitation over Nepal, presented in Fig. 2c. The result shows that the precipitation is highly variable in the country, especially in the western and central regions. In contrast, the interannual precipitation variability is less variable in the eastern region, with low precipitation values (Fig. 2c). Likewise, the precipitation distribution, the interannual rainfall variability gradually decreases from west to east.

The spatial trend of winter precipitation based on APHRODITE data in Fig. 3a shows a significant increasing trend at a rate of 0.95 mm/year over the high-land areas of the western and central regions. The decreasing trend (insignificant) is also observed in the mid-elevation areas of the western region, a similar pattern is also evident in the study

of Wang et al. (2013). The upward trend and downward or no trend areas are located at high-precipitation and low-precipitation areas, as observed in Fig. 2a, respectively, indicating precipitation is decreasing (increasing) over those areas with high (low)-precipitation. Additionally, we have also used ERA5 data to demonstrate the spatial trend of the winter precipitation in Fig. 3b. ERA5 shows a different trend than APHRODITE, with an increasing trend over the country with a significant increasing trend over the central region and mid-elevation areas of the eastern region. The higher increment rate in ERA5 data than in APHRODITE data might be related to the overestimation of the observed precipitation amount, as mentioned in the earlier studies of Sharma et al. (2020a) and Chen (2021).

3.2 Temporal Variability

The trend analysis of the winter precipitation shows no significant trend over regional and national scales; however, considerable interannual variability is more evident during 1960–2015 (Fig. 4). The winter precipitation amount is very low and mostly occurs in the form

of snow, especially in the highlands of the western and central region (Pokharel et al. 2019). Moreover, the time series has a similar variation of the precipitation between three sub-regions and over the country. Further, we have

separated the wet and dry years during the study period based on the standardized anomalies of ≥ 1 and ≤ -1 , respectively (Table 1). Below-normal precipitation (dry years) is more evident before 1980. In contrast, the

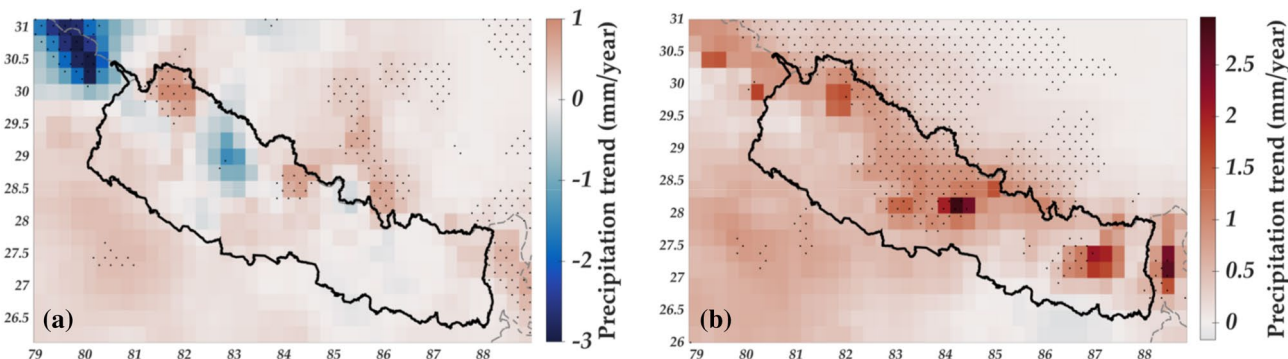


Fig. 3 Spatial trend (mm/year) for the winter season (DJF) in **a** APHRODITE and **b** ERA5 data from 1960 and 2015. The black dot represents the significance at a 95% confidence level

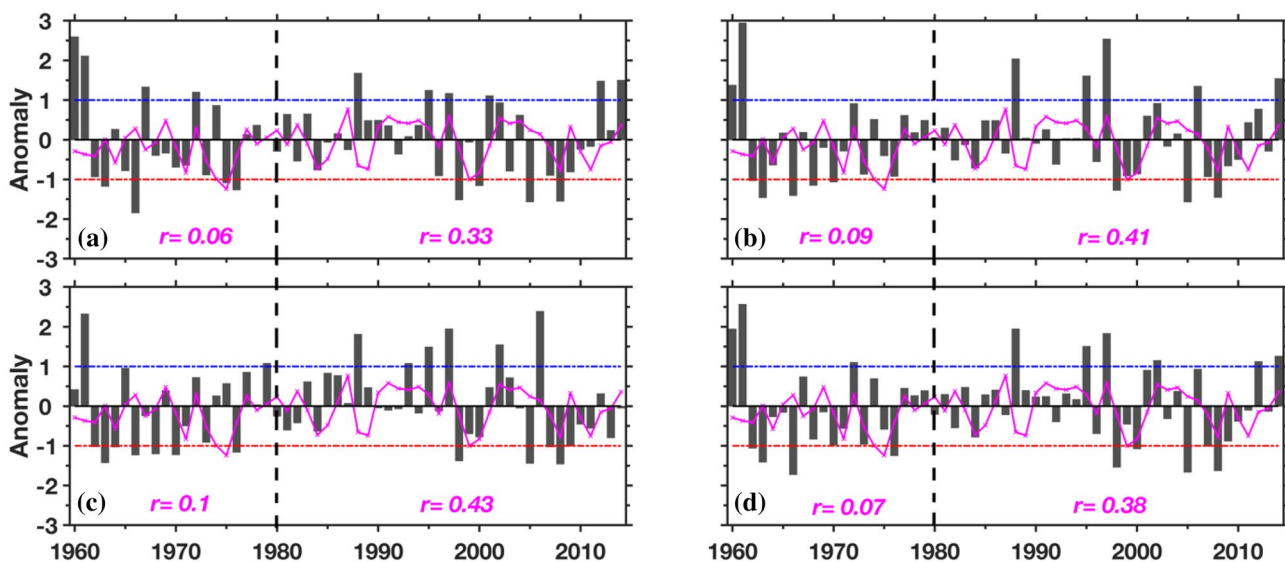


Fig. 4 Time series of the average precipitation (gray bar) during 1960–2015 over **a** Western, **b** Central, **c** Eastern regions, and **d** Nepal with NINO3.4 SST anomaly (magenta line). Blue and red dotted line represents the wet and dry threshold, respectively. Black dot

line separates the correlation period. r value represents the correlation between winter precipitation and NINO3.4 SST anomaly for the respective period (before and after 80 s)

Table 1 Separation of the dry and wet years during 1960–2015 over Nepal and different regions

Regions	Dry years	Occurrence (%)	Wet years	Occurrences (%)
Western	1963, 1966, 1975, 1976, 1998, 2000, 2005, 2008	15	1960, 1961, 1967, 1972, 1988, 1995, 1997, 2001, 2012, 2013	18
Central	1962, 1963, 1966, 1968, 1970, 1998, 2005, 2008	16	1960, 1961, 1988, 1995, 1997, 2006, 2014	13
Eastern	1962, 1963, 1964, 1966, 1968, 1970, 1976, 1998, 2005, 2007, 2008	20	1961, 1979, 1988, 1993, 1995, 1997, 2002, 2006	15
Nepal	1962, 1963, 1966, 1976, 1998, 2005, 2007, 2008	15	1960, 1961, 1972, 1988, 1995, 1997, 2002, 2012, 2014	16

opposite precipitation pattern (shifted to the above-normal (wet years)) was observed after 1980 and continued up to the 1990s.

As, the opposite pattern in winter precipitation is observed, the NINO3.4 SST anomaly is also plotted to analyze the influence during the study period (Fig. 4). Similar to the study of Yadav et al. (2010), the influence of the ENSO is also changed before and after the 1980s. Additionally, we have also calculated the correlation between NINO3.4 SST anomaly and winter precipitation for before and after the 1980s and found that small correlation ($r \leq 0.1$) before 1980, while a relatively higher correlation ($r \geq 0.33$) after 1980. This variation in the SST pattern can be linked to the variation in dry and wet years during the winter season throughout the study period.

Likewise, the country also witnessed many dry years between 2000 and 2010. The results show a higher degree of variability after the 1990s. Further, the total occurrence of the wet (dry) years over the western, central, and eastern regions were 18 (15%), 13 (16%), and 15 (20%), respectively, during the study period. The frequency of the dry and wet years is slightly higher in the eastern and central regions, respectively, during the study period (Table 1). Overall, at

the national scale, the frequency of dry and wet years is very similar (nominal difference in wet and dry years).

3.3 Dominant Pattern of Variability

As the variability of dry and wet years was observed over the country; thus, the long-term detrended winter precipitation during 1960–2015 were passed through EOF analysis. The dominant modes of winter precipitation are presented in Fig. 5a, b. Two dominant modes can explain the maximum winter precipitation variability over Nepal and are isolated from the other modes (North et al. 1982). The first two EOF modes can explain about 61.8% of the total variance, with the leading EOF1 mode capturing 42.9% of the variance, while the EOF2 contributes 18.9% of the total variance. Figure 4a shows the uniform signal over the entire study region giving a monopole pattern of variability, with strong loadings over the western and central regions, whereas the heterogeneous pattern of the winter precipitation was observed in the EOF2 (Fig. 5b).

The standardized principal components (PC1 and PC2) associated with EOFs are displayed in Fig. 5c, d. The PC1 gives the interannual precipitation variability over Nepal

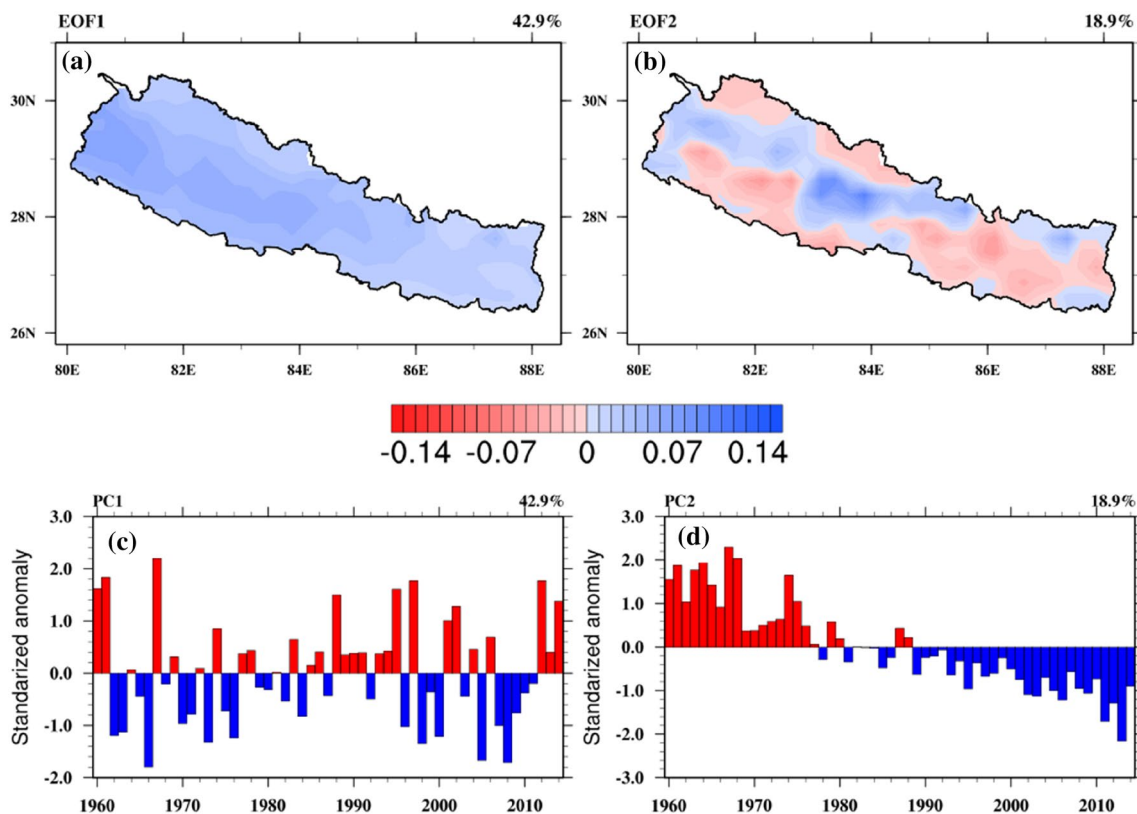


Fig. 5 a EOF1 and b EOF2 and their respective c PC1 and d PC2 of the winter precipitation during 1960–2015 in Nepal. The first (EOF1) and second (EOF2) dominant mode of variability explains 42.9% and

18.9% of the total variance of the mean winter precipitation, respectively. EOF pattern is expressed in percentage

from 1980 to 2015 (Fig. 4c). The lowest winter precipitation years in PC1 were 1962, 1963, 1996, 1973, 1976, 1996, 1998, 2000, 2005, 2007, and 2008. Similarly, the highest precipitation years were 1960, 1961, 1967, 1988, 1995, 1997, 2001, 2002, 2012, and 2014. Further, the positive precipitation anomalies shifted to the negative precipitation anomalies, showing decadal variability after the 1990s in PC2 (Fig. 5d). Likewise, Huang et al. (2017) and Choi et al. (2016) also reported a similar interdecadal change in the winter precipitation over the northern slope of central Himalaya (Southern China).

3.4 Relationship with Oceanic Pattern

Figure 6 shows the statistical relationship between SST and the dominant modes of winter precipitation, explaining the

influences of SST on respective EOFs. The simultaneous SST distribution concerning PC1 shows that the SST anomalies are more robust over the Pacific Ocean, giving characteristics of the ENSO pattern, with anomalous positive SST in the mid-eastern Pacific Ocean and negative SST anomalies in the western tropical Pacific (Fig. 6a). Moreover, the positive SST signal over the Indian Ocean is robust and significant at the 90% confidence level. Further, the correlation between PCs and SST indices (NINO3.4, IOBM, and NAO) is presented in Table 2. The correlation between PC1 and NINO3.4 and IOBM shows the significant influence of both SST indices on winter precipitation. Similarly, coherent variation of the ENSO and basin-wide Indian Ocean SST has been also reported by Liu et al. (2020).

However, NAO does not significantly influence the PC1, suggesting the first mode of winter precipitation variability

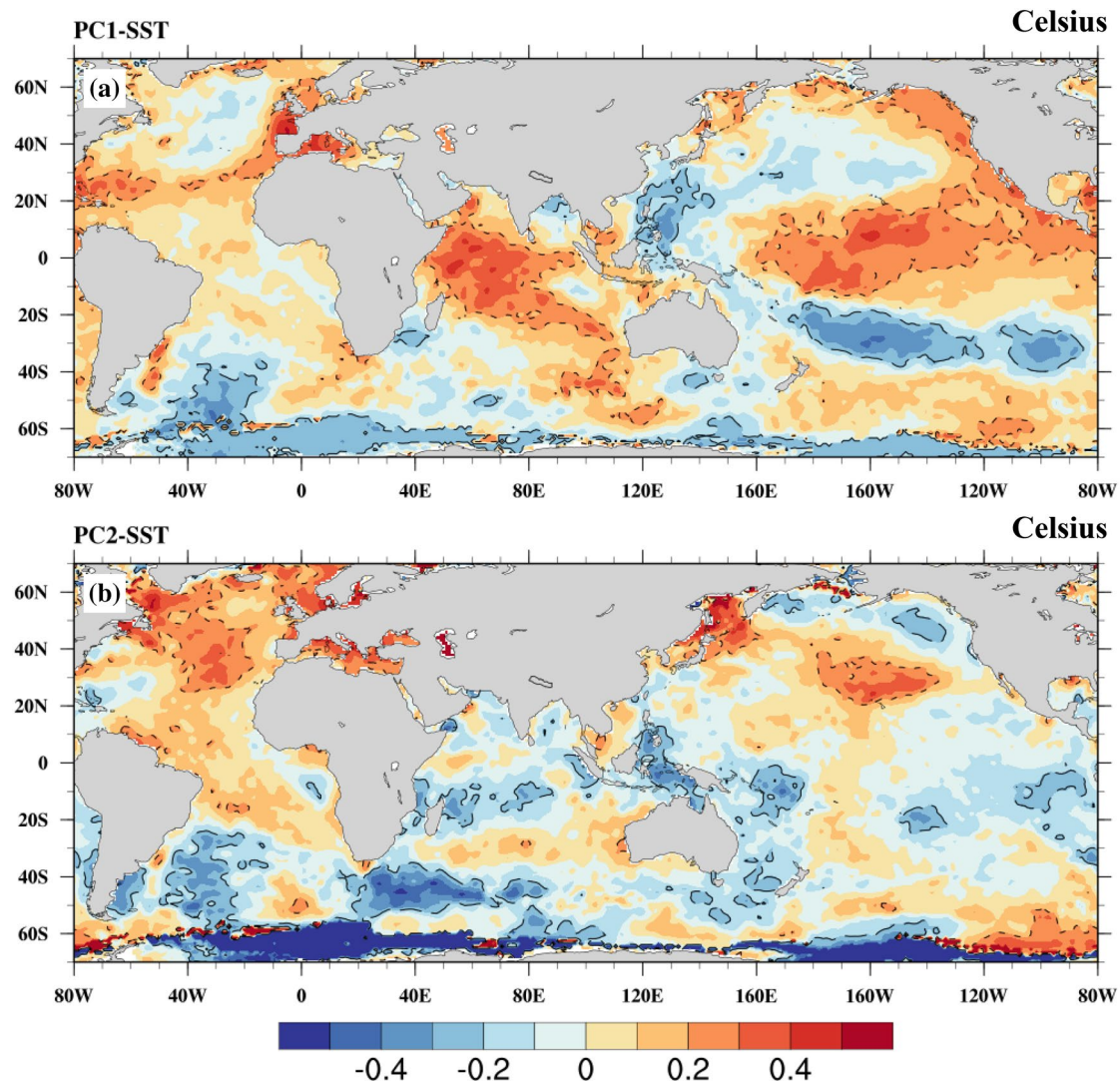


Fig. 6 The correlation of SST (unit: °C) with **a** PC1 and **b** PC2 during 1960–2015. The dotted line represents the significance at a 90% confidence interval

Table 2 Correlation of PCs with NINO3.4, DMI, and NAO

Precip/PCs	NINO3.4	IOBM	NAO
Nepal	0.25*	0.28*	0.17
Western	0.23*	0.24*	0.15
Central	0.27*	0.29*	0.19
Eastern	0.28*	0.30*	0.17
PC1	0.25*	0.27*	0.15
PC2	0.04	0.05	0.43*

The * represents the significant at a 90% confidence interval

is related to the SST anomalies over the Pacific and the Indian Oceans. This pattern is consistent with the interannual variation of the leading mode of precipitation over China and Northern India related to ENSO and IOBM (Kar and Rana 2014; Liu et al. 2020; Zhou 2019). Further, Hamal et al. (2020a) suggested that SST anomalies over the Pacific and the Indian Ocean affect the convection, surface air temperature, and wind circulation, affecting moisture transport to the area of interest.

The correlation of the PC2 with SST anomalies is presented in Fig. 6b. The most significant signals are observed over the Pacific and the Indian Ocean, however, not strong as PC1. In the Northern Atlantic Ocean, there are widespread significant positive anomalies. Moreover, the correlation between PC2 and NAO is 0.43 (significant at a 90% confidence interval), suggesting the North Atlantic Ocean SST may influence the EOF2 of winter precipitation by modulating the NAO pattern (Table 2). Moreover, PC2 has a weak and non-significant correlation with NINO3.4 and IOBM, indicating that this mode is independent of SST anomalies in the Indian and Pacific Oceans. This overall weak correlation is due to the changing phase of ENSO before and after 1980 (as observed in Fig. 4). Further, Kar and Rana (2014) found that the NAO's influence on the winter time precipitation over northwest India is more prominent in amplitude in PC2 than ENSO.

3.5 Relationship with Atmospheric Circulation

To provide associated features of the large-scale circulation with the different modes of winter precipitation, the correlation with stream function is presented in Fig. 7. The PC1 with mid-level stream function shows a positive correlation over the tropical Indian Ocean and a negative correlation over western Himalayan, Tibetan Plateau, and Nepal (Fig. 7a). The wet condition is observed beneath the cyclonic circulation, so the same precipitation pattern over Nepal in EOF1. Moreover, the divergent circulation (anticyclone circulation) over the Indian Ocean may initiate the moisture

transport to Nepal, as observed in the earlier study (Hamal et al. 2020a).

The correlation of the PC2 and stream function anomalies at the mid-level shows a strong positive relationship with the North Atlantic Ocean (Fig. 7b). Moreover, it has a pair of anticyclones centered at 25°N, showing that the North Atlantic Ocean modulates the wave train and propagates eastward to the western Himalayas. The correlation further shows that ENSO is inactive in the PC2; however, it corresponds well with the NAO pattern.

In the winter season, the moisture transport from the Arabian Sea and western IO are the prime sources, and divergence of the moisture is more prominent around the study region (Dimri 2013a). Previously, several studies have shown that interannual variability of winter storm occurrences is well correlated with the polar/Eurasia teleconnections pattern (Lang and Barros 2004); which relates to other large-scale natural climate variabilities, such as the Arctic Oscillation (AO) and the North Atlantic Oscillation (NAO), to the winter climate of Nepal. The Equatorial wind systems seem to relate SST anomalies of the African coast with moisture flux from the Arabian Sea to Indian continental region, including Nepal. Further, the above normal SST over the equatorial Indian Ocean is related to the high winter precipitation in Nepal, while below normal precipitation is related with negative DMI and positive SOI (Yadav et al. 2007).

4 Conclusion

Winter precipitation only contributes ~5% to annual precipitation; however, it has great importance to agriculture, glacier mass balance, water resource management, and the socio-economy of the country. Thus, this study investigates the long-term variability of winter precipitation during 1960–2015 over the southern slope of Central Himalaya, Nepal. The climatological mean during the study period shows their highest values in the western region and decreases eastward with minimum precipitation in the eastern region. Further, the spatial trend shows the upward trend (below 1 mm/year) over the highlands of western and central region, whereas decreasing or no trend is observed over the most of the areas. As the influence of the ENSO changed after and before 1980, the below-normal precipitation is more evident before 1980, while the pattern shifted to the above-normal after 1980 and continued up to the 1990s before the occurrence of many dry years between 2000 and 2010.

The dominant mode of the winter precipitation and their association with the SST and stream function anomalies at interannual timescale shows two dominant modes of winter

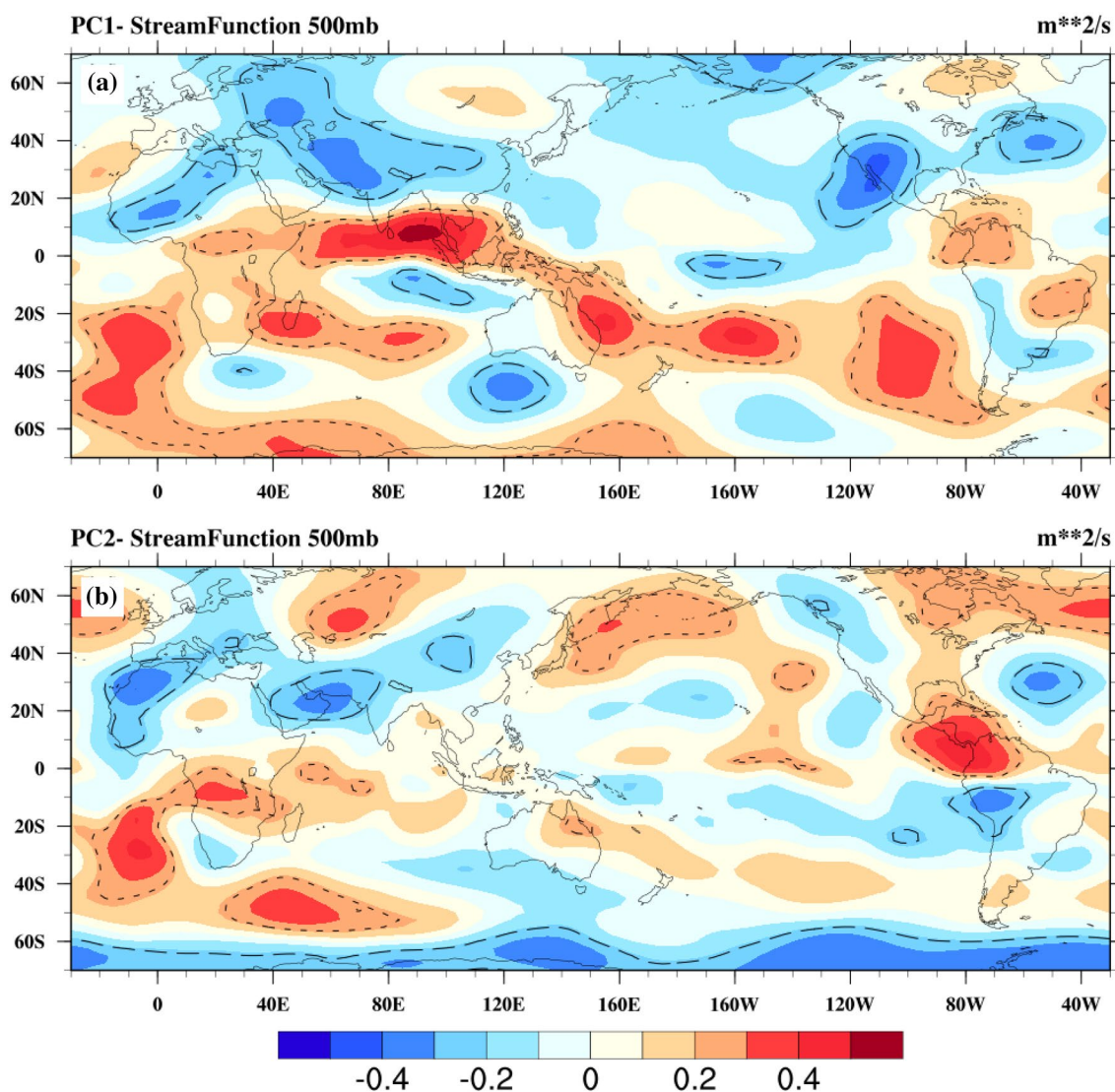


Fig. 7 The correlation of stream function (unit: m^2/s) with **a** PC1 and **b** PC2 during 1960–2015. The dotted line represents the significance at a 90% confidence interval

precipitation over Nepal. The first mode of EOF shows the monopole pattern of precipitation variability over the study region, capturing 42.9% of the variance. The EOF1 is mainly associated with remotely ENSO, which local influences are seen through the Indian Ocean teleconnection. The heterogeneous precipitation variability pattern was observed in the second mode of EOF, which contributed 18.9% of the total variance. The North Atlantic Ocean's impact was observed on the EOF2 that modulates the mid-latitudes wave train and propagates eastward to the Western Himalayas. The result indicates that the tropical Indian, Pacific, and Atlantic are the primary sources of winter precipitation variability and predictability in Nepal.

Acknowledgements We acknowledge the gridded data availability from APHRODITE, and ECMFW. The first author BD, invited visiting professor at Interdisciplinary Centre for Mountain Research (CIRM), University of Lausanne, Switzerland, is thankful to University of Lausanne for invitation and Herbette Foundation for the support of this visit.

Funding This research did not receive any internal and external funding. This research is conducted independently from the authors as a part of their research and study. The organization and institution mentioned in the study have no role in the design and funding of the study.

Data Availability Gridded Asian Precipitation—Highly-Resolved Observational Data Integration Towards Evaluation Version 1 and 2 (APHRODITE-v01 and v02) datasets used in this study can be freely accessed from <http://www.aphrodite.st.hirosaki-u.ac.jp/>. ERA5 reanalysis data can be freely accessed from <https://www.cds.climate.copernicus.eu/>.

Declarations

Conflict of Interest The authors declare that they have no conflict of interest.

References

- Abid MA, Ashfaq M, Kucharski F, Evans KJ, Almazroui M (2020) Tropical Indian Ocean mediates ENSO influence over central southwest Asia during the wet season. *Geophys Res Lett* 47:e2020GL089308
- Barlow M, Cullen H, Lyon B (2002) Drought in central and southwest Asia: La Niña, the warm pool, and Indian Ocean precipitation. *J Clim* 15:697–700
- C3S (2017) ERA5: Fifth generation of ECMWF atmospheric reanalyses of the global climate. Copernicus Climate Change Service Climate Data Store (CDS), November, 2019. <https://www.cds.climate.copernicus.eu/cdsapp#!/home>. Accessed Dec 2021
- Chen Y, Coauthors (2021) Spatial performance of multiple reanalysis precipitation datasets on the southern slope of central Himalaya. *Atmos Res* 250:105365
- Choi J-W, Lee S-W, Lim B-H, Kim B-J (2016) Interdecadal change of winter precipitation over southern China in late 1990s. *J Meteorol Soc Jpn Ser II* 94:197–213
- Dey D, Döös K (2019) The coupled ocean–atmosphere hydrologic cycle. *Tellus A* 71:1650413
- Dimri AP (2013a) Relationship between ENSO phases with Northwest India winter precipitation. *Int J Climatol* 33:1917–1923
- Dimri AP (2013b) Interannual variability of Indian winter monsoon over the Western Himalayas. *Global Planet Change* 106:39–50
- Hamal K, Sharma S, Baniya B, Khadka N, Zhou X (2020a) Inter-annual variability of winter precipitation over nepal coupled with ocean-atmospheric patterns during 1987–2015. *Front Earth Sci* 8:161
- Hamal K, Sharma S, Khadka N, Haile GG, Joshi BB, Xu T, Dawadi B (2020b) Assessment of drought impacts on crop yields across Nepal during 1987–2017. *Meteorol Appl* 27:e1950
- Hasson S, Lucarini V, Khan MR, Petitta M, Bolch T, Gioli G (2014) Early 21st century snow cover state over the western river basins of the Indus River system. *Hydrol Earth Syst Sc* 18:4077–4100
- Huang D, Dai A, Zhu J, Zhang Y, Kuang X (2017) Recent winter precipitation changes over eastern China in different warming periods and the associated East Asian jets and oceanic conditions. *J Clim* 30:4443–4462
- Huber DG, Gullede J (2011) Extreme weather and climate change: understanding the link, managing the risk. Pew Center on Global Climate Change Arlington, Arlington
- Hunt KM, Zaz SN (2022) Linking the North Atlantic Oscillation to winter precipitation over the Western Himalaya through disturbances of the subtropical jet. *Clim Dynamics*. <https://doi.org/10.1007/s00382-022-06450-7>
- Kamil S, Almazroui M, Kang I-S, Hanif M, Kucharski F, Abid MA, Saeed F (2019) Long-term ENSO relationship to precipitation and storm frequency over western Himalaya–Karakoram–Hindukush region during the winter season. *Clim Dyn* 53:5265–5278
- Kansakar SR, Hannah DM, Gerrard J, Rees G (2004) Spatial pattern in the precipitation regime of Nepal. *Int J Climatol* 24:1645–1659
- Kar SC, Rana S (2014) Interannual variability of winter precipitation over northwest India and adjoining region: impact of global forcings. *Theoret Appl Climatol* 116:609–623
- Lang TJ, Barros AP (2004) Winter storms in the central Himalayas. *J Meteorol Soc Jpn Ser II* 82:829–844
- Liu X, Chen B (2000) Climatic warming in the Tibetan Plateau during recent decades. *Int J Climatol* 20:1729–1742
- Liu Y, Hu Z-Z, Wu R (2020) Cooperative effects of tropical Pacific and Atlantic SST forcing in southern China winter precipitation variability. *Clim Dyn* 55:2903–2919
- Lorenz EN (1956) Empirical orthogonal functions and statistical weather prediction. Massachusetts Institute of Technology, Department of Meteorology Cambridge, Cambridge
- Lu B, Coauthors (2019) Impact of El Niño and Southern Oscillation on the summer precipitation over Northwest China. *Atmos Sci Lett* 20:e928
- Mehmood S, Coauthors (2022) Dominant controls of cold-season precipitation variability over the high mountains of Asia. *npj Clim Atmos Sci* 5:1–13
- Mishra V, Smoliak BV, Lettenmaier DP, Wallace JM (2012) A prominent pattern of year-to-year variability in Indian Summer Monsoon Rainfall. *Proc Natl Acad Sci USA* 109:7213–7217
- Nayava JL (1980) Rainfall in Nepal. *Himal Rev* 12:1–18
- Niranjan Kumar K, Rajeevan M, Pai DS, Srivastava AK, Preethi B (2013) On the observed variability of monsoon droughts over India. *Weather Clim Extrem* 1:42–50
- North GR, Bell TL, Cahalan RF, Moeng FJ (1982) Sampling errors in the estimation of empirical orthogonal functions. *Mon Weather Rev* 110:699–706
- Pokharel B, Wang SYS, Meyer J, Marahatta S, Nepal B, Chikamoto Y, Gillies R (2019) The east–west division of changing precipitation in Nepal. *Int J Climatol* 40:3348–3359
- Sein ZMM, Ogwang B, Ongoma V, Ogou FK, Batebana K (2015) Inter-annual variability of May–October rainfall over Myanmar in relation to IOD and ENSO. *J Environ Agric Sci* 4:28–36
- Sharma S, Hamal K, Khadka N, Joshi BB (2020a) Dominant pattern of year-to-year variability of summer precipitation in Nepal during 1987–2015. *Theoret Appl Climatol* 142:1071–1084
- Sharma S, Khadka N, Hamal K, Baniya B, Luintel N, Joshi BB (2020b) Spatial and temporal analysis of precipitation and its extremities in seven provinces of Nepal (2001–2016). *Appl Ecol Environ Sci* 8:64–73
- Sharma S, Coauthors (2021) Projected drought conditions over southern slope of the Central Himalaya using CMIP6 models. *Earth Syst Environ* 5:1–11
- Syed F, Giorgi F, Pal J, King M (2006) Effect of remote forcings on the winter precipitation of central southwest Asia part 1: observations. *Theoret Appl Climatol* 86:147–160
- Syed FS, Giorgi F, Pal J, Keay K (2010) Regional climate model simulation of winter climate over Central-Southwest Asia, with emphasis on NAO and ENSO effects. *Int J Climatol* 30:220–235
- Wang S-Y, Yoon J-H, Gillies RR, Cho C (2013) What caused the winter drought in Western Nepal during recent years?*,+. *J Clim* 26:8241–8256
- Wang L, Chen W, Zhou W, Huang G (2015a) Teleconnected influence of tropical Northwest Pacific sea surface temperature on interannual variability of autumn precipitation in Southwest China. *Clim Dyn* 45:2527–2539
- Wang X, Cui G, Wu F, Li C (2015b) Analysis of temporal-spatial precipitation variations during the crop growth period in the Lancang River basin, southwestern China. *Ecol Eng* 76:47–56
- Yadav RK, Rupa Kumar K, Rajeevan M (2007) Role of Indian Ocean Sea surface temperature in modulating northwest Indian winter precipitation variability. *Theor Appl Climatol* 87:73–83
- Yadav R, Rupa KK, Rajeevan M (2009) Increasing influence of ENSO and decreasing influence of AO/NAO in the recent decades over northwest India winter precipitation. *J Geophys Res*. <https://doi.org/10.1029/2008JD011318>
- Yadav RK, Yoo JH, Kucharski F, Abid MA (2010) Why is ENSO influencing northwest India winter precipitation in recent decades? *J Clim* 23:1979–1993

- Yadav R, Ramu D, Dimri A (2013) On the relationship between ENSO patterns and winter precipitation over North and Central India. *Global Planet Change* 107:50–58
- Yatagai A, Arakawa O, Kamiguchi K, Kawamoto H, Nodzu MI, Hamada A (2009) A 44-year daily gridded precipitation dataset for Asia based on a dense network of rain gauges. *SOLA* 5:137–140
- Yatagai A, Kamiguchi K, Arakawa O, Hamada A, Yasutomi N, Kitoh A (2012) APHRODITE: constructing a long-term daily gridded precipitation dataset for Asia based on a dense network of rain gauges. *Bull Am Meteor Soc* 93:1401–1415
- Zhang Z, Moore JC (2015) Chapter 6—Empirical orthogonal functions. *Mathematical and physical fundamentals of climate change*. Elsevier, Amsterdam, pp 161–197
- Zhang L, Fraedrich K, Zhu X, Sielmann F, Zhi X (2015) Interannual variability of winter precipitation in Southeast China. *Theoret Appl Climatol* 119:229–238
- Zhou L-T (2019) Dominant modes of wintertime precipitation variability in arid and semi-arid region of Northwest China. *AGU Fall Meeting Abstracts*, H11N-1704

Springer Nature or its licensor (e.g. a society or other partner) holds exclusive rights to this article under a publishing agreement with the author(s) or other rightsholder(s); author self-archiving of the accepted manuscript version of this article is solely governed by the terms of such publishing agreement and applicable law.